

Laser Heater and seeded Free Electron Lasers

G. Dattoli* and E. Sabia†

*ENEA - Centro Ricerche Frascati, via E. Fermi,
45, IT 00044 Frascati (Roma), Italy*

V. Petrillo‡

*INFN - Milano and Università di Milano,
via Celoria, 16 20133 Milano, Italy*

Abstract

In this paper we consider the effect of laser heater on a seeded Free Electron Laser. We develop a model embedding the effect of the energy modulation induced by the heater with those due to the seeding. The present analysis is compatible with recent experimental results and earlier predictions displaying secondary maxima with increasing heater intensity. The treatment developed in the paper confirms and extends the previous analyses and put in evidence further effects which can be tested in future experiments.

PACS numbers:

Keywords:

*Electronic address: giuseppe.dattoli@enea.it

†Electronic address: elio.sabia@enea.it

‡Electronic address: vittoria.petrillo@mi.infn.it

I. INTRODUCTION

Laser Heater (LH) has been proven to be a key element for Self Amplified Spontaneous Emission Free Electron Laser (SASE-FEL) operation with high brightness e-beams [1].

The concepts underlying LH trace back to the seminal papers in refs. [2, 3], where it was pointed out that the onset of instabilities, like those due to coherent synchrotron radiation (CSR) [4], can be counteracted by a FEL type interaction with an external laser. The induced energy spread reduces the gain of the instability, thus preventing its growth. The associated physical mechanism can therefore be ascribed to a manifestation of the Landau damping, already invoked in the past to account for the experimentally observed competition between the FEL and the microwave instability in Storage Ring (SR) devices [5]. In SR FEL the effect induced by the laser growth on the microwave instability (and vice-versa) is fairly complex and can be modeled by merging the equations ruling the evolution of the two instabilities (FEL and microwave). The final result is the derivation of a system of non-linear set of differential equations resembling those of the Volterra prey-predator model, thus getting a fairly transparent understanding of the dynamics of the competition. In the case of SR-FEL the mechanism of the competition is self-regulatory, laser and instability reach a kind of compromise allowing the coexistence.

In the case of LH, being the laser inducing the beam heating an external device, the question arises on what should be the amount of laser intensity to avoid a significant disruption of the quality of the e-beam, which in turn may prevent the SASE FEL operation.

We expect therefore that, as shown in Fig. 1, the output laser intensity increases, with the heater power, until the induced Landau damping is able to control the instability growth beam energy, on the other side the FEL power decreases when the FEL induced energy spread dominates the heater process [6].

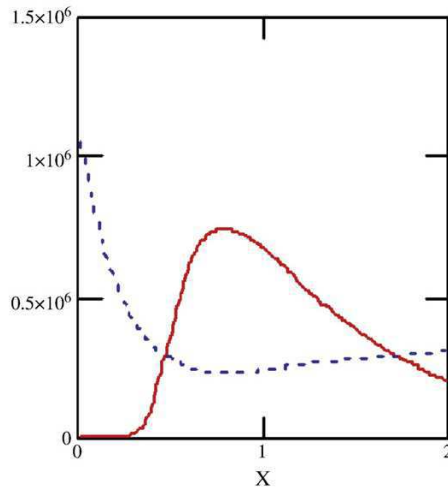


FIG. 1: FEL intensity (continuous line) and e-beam energy spread (dotted line) vs. the laser heater power (for the specification of the units see section III).

Recent experimental results [7] have confirmed such a “paradigm” and have displayed further and interesting physics when heater is combined with a seeded operation.

The new features emerging from these studies are displayed in Figs. 3 and 4 of ref. [7], which show that secondary maxima appear, for large values of the heater energy.

This effect was predicted in ref. [2], where it was suggested that the underlying physical mechanisms are essentially due to the peculiar nature of the energy distribution acquired by the e-beam after the heater interaction which does not remain Gaussian anymore.

In this paper we will reconsider the problem ab-initio, by developing a numerical code based on the solution of the Liouville equation, which governs the phase space evolution of the e-beam undergoing three different manipulation stages summarized in Fig. 2: Heating, Acceleration, Seeding. The novelty of our results relies on the numerical technique we employ. It allows comprehensive treatment of the problem, yielding the full dependence of the effect at low and high heater energy and the inclusion of odd and even harmonics as well. The latter seem characterized by different behaviors, which could be tested in future experimental investigations.

The main achievement of the present analysis is the evaluation of the bunching coefficients, determined in the modulator by the seeding process. The model we develop has the advantage of reproducing the behavior at low and large heater energy, by covering correctly

the region before the first peak characterizing the bunching coefficients.

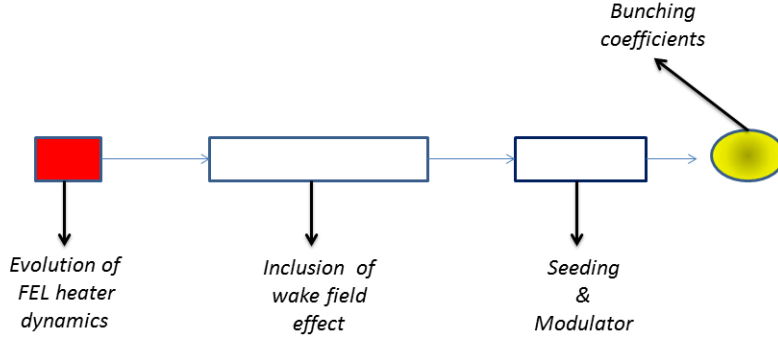


FIG. 2: Flow chart of the procedure adopted

II. THE MODEL

We model the evolution of the FEL-Heater-Seeded device by first solving the Liouville equation yielding the e-beam phase space distribution ρ after that the electrons have undergone the heating process, according to the sketch in Fig. 2.

The Liouville equation we will consider is given below [8]

$$\begin{aligned} \frac{\partial}{\partial \tau} \rho &= -\nu \frac{\partial}{\partial \zeta} \rho + |a| \cos(\zeta) \frac{\partial}{\partial \nu} \rho, \\ \rho(\nu, \zeta) |_{\tau=0} &= f(\nu) \end{aligned} \quad (2.1)$$

where ν, ζ are the e-beam phase space variable, τ the dimensionless time and $|a|$ is the Colson

FEL dimensionless amplitude [9]. The function $f(\nu)$, representing the initial condition of our Cauchy problem, is the energy distribution of the e-beam at the entrance of the heater.

Eq. (2.1) has been integrated using a symplectic leapfrog scheme [10] with $f(\nu)$ being a Gaussian. Such a functional form is roughly preserved for modest values of the heater energy, but, when it increases, the distribution is distorted and secondary lobes appear [9] (see Fig. 3).

Being not interested into the details of the CSR inside the LINAC, we use a standard procedure (described e. g. in [2]), modelling the effect of the heater through the wake field

induced energy spread.

The total energy spread (CSR + Heater) vs. the heater energy, at the entrance of the modulator, is shown in Fig. 4, the behaviour is easily understandable. After a damping of the instability, the laser induced energy spread becomes dominant and the total energy spread increases.

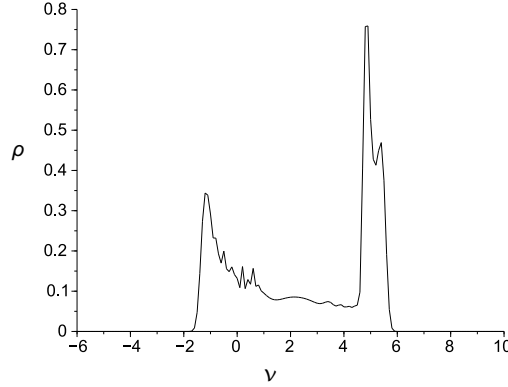


FIG. 3: Energy distribution distortion at $|a|^2 = 16$

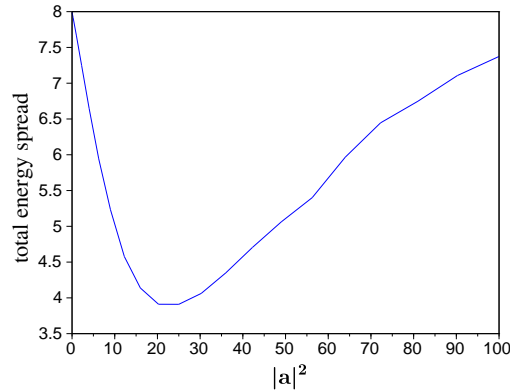


FIG. 4: Total energy spread (CSR+ Heater) vs. $|a|^2$.

We have modelled the e-beam phase space evolution in the modulator using the same Liouville equation in eq. (2.1), in which $|a|$ is replaced by the seed amplitude and the phase space variables are rescaled according to the new parameters (the average beam energy and the undulator geometry). The energy distribution is assumed to be that calculated with the combined effect of Heater and CSR. The previously adopted solution procedure

of the Liouville equation yields the e-beam phase space distribution at the entrance of the modulator. We can therefore expand the phase space distribution in a Fourier series, namely

$$\rho(\nu, \zeta) = \sum_n b_n e^{in\zeta} \quad (2.2)$$

and then we evaluate the bunching coefficients b_n as

$$b_n(\nu) = \frac{1}{2\pi} \int_0^{2\pi} \rho(\nu, \zeta) e^{-in\zeta} d\zeta \quad (2.3)$$

By taking a further average on the energy distribution, we obtain what is shown in Figs. 5, regarding the energy averaged bunching coefficients ($n = 3, 13$) vs. the heater energy. The case $n=2$ is reported in Fig. 6. The horizontal axis in the previous figures is expressed in terms of the dimensionless amplitude $|a|^2$, which is in turn related to the heater energy. We have used dimensionless unit rather than dimensional because we prefer to provide general trends which can be later adapted to a more specific experimental configuration as we will see in the following. A rescaling of the dimensionless amplitude in terms of heater energy will be discussed in the concluding section of this paper.

The behavior is paradigmatically similar for all the harmonics: a growth, a maximum, a decrease, new secondary maxima. The larger harmonic number corresponds to a more significant sensitivity of the maxima to the heater energy, which is reflected by a narrower peak and by a smaller peak to peak ratio.

The even harmonic $n = 2$ displays a more intrigued pattern providing a secondary maximum larger than the first.

The first maxima are obtained in correspondence of the minimum of the total energy spread (Fig. 6), the secondary maxima are associated with a more complicated dynamical behaviour we will discuss below.

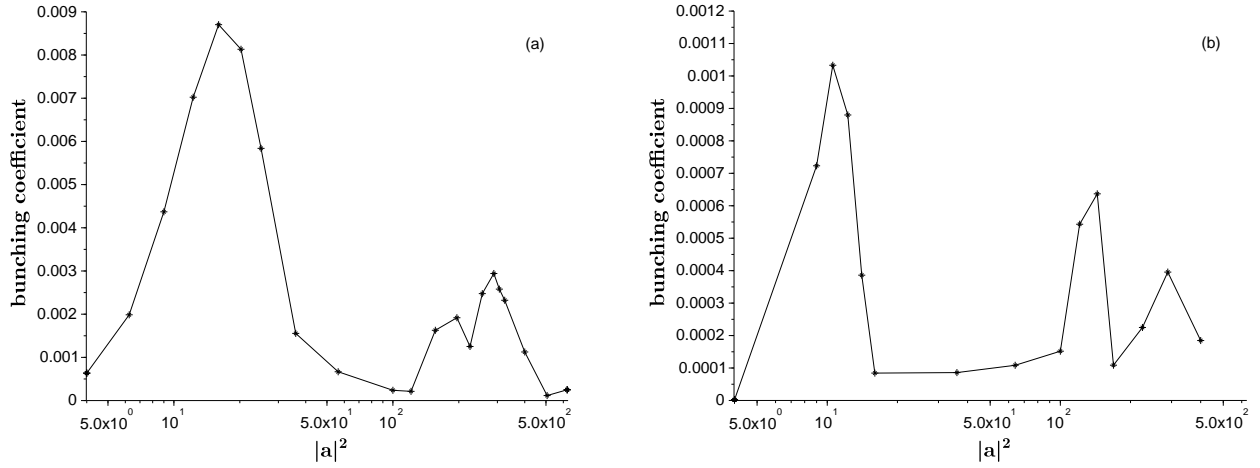


FIG. 5: Bunching coefficients at the end of the modulator vs. $|a|^2$, (a) $n=3$, (b) $n=13$.

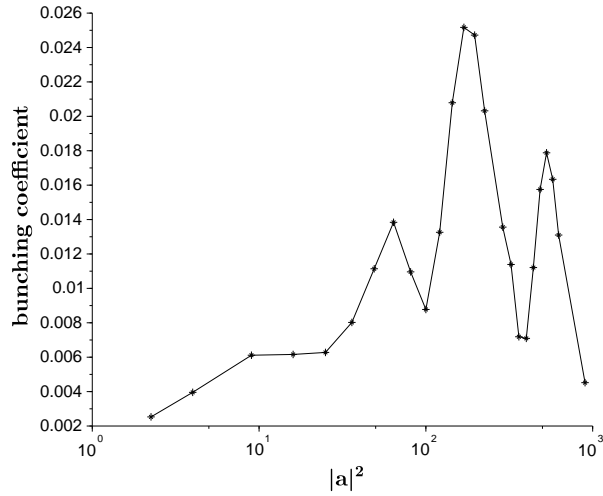


FIG. 6: Same of Fig. 5 for $n=2$

In Fig. 7 we show the position of the maxima and the total energy spread vs. the heater energy. It is worth stressing that the first maxima of the odd harmonics are all in correspondence (even though not exactly the same) of the minimum of the total energy spread, the secondary maxima (including those of the second harmonic) are shifted towards the region in which the heater induced energy spread is dominating with respect to the CSR spread. It must be stressed that in this region of the heater energy, the energy distribution at the entrance of the modulator is far from being a Gaussian and the energy spread (considered

as the r.m.s. of the distribution) cannot be considered fully representative of the whole distribution.

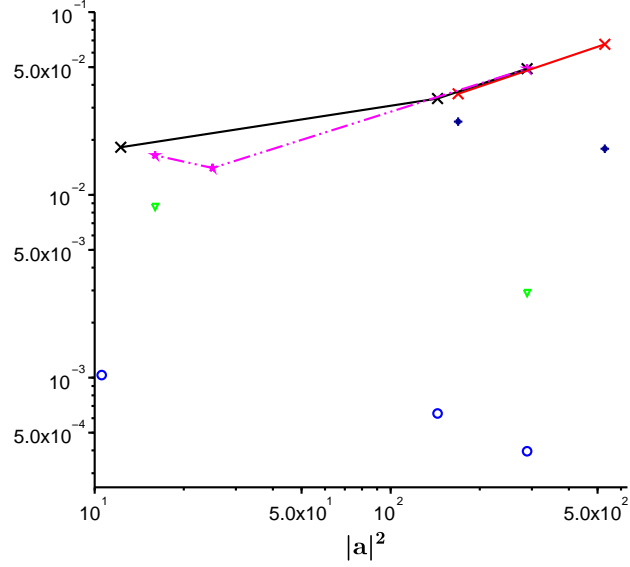


FIG. 7: Bunching coefficient peak position $n=3$ (green triangle mark), $n=13$ (blue circle mark), $n=2$ (black diamond mark) vs. $|a|^2$, the interpolating line refers to the heater induced energy spread

In Figs. 9-10 we have reported the energy distribution at the entrance of the modulator and at the end of the modulator for different values of the dimensionless seeding amplitude $|a|$, corresponding to the position of the first and second maxima of the bunching coefficient $n = 3$.

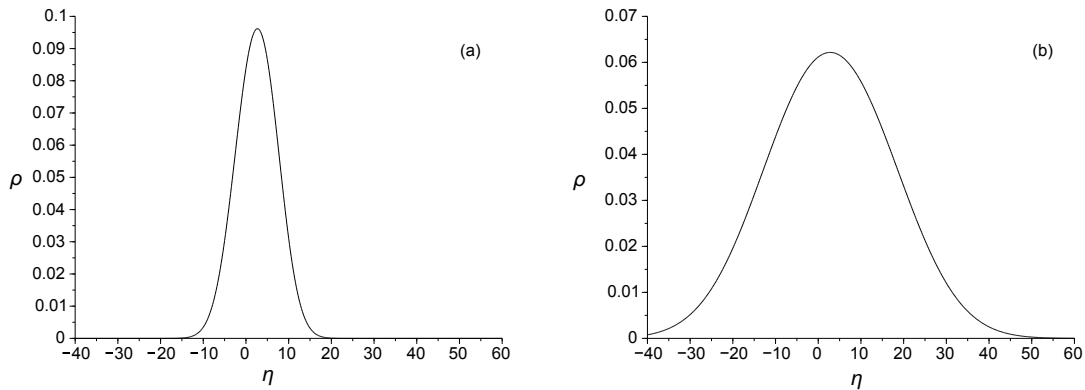


FIG. 8: Energy distribution at the entrance of the modulator for (a) $|a|^2 = 16$, (b) $|a|^2 = 289$.

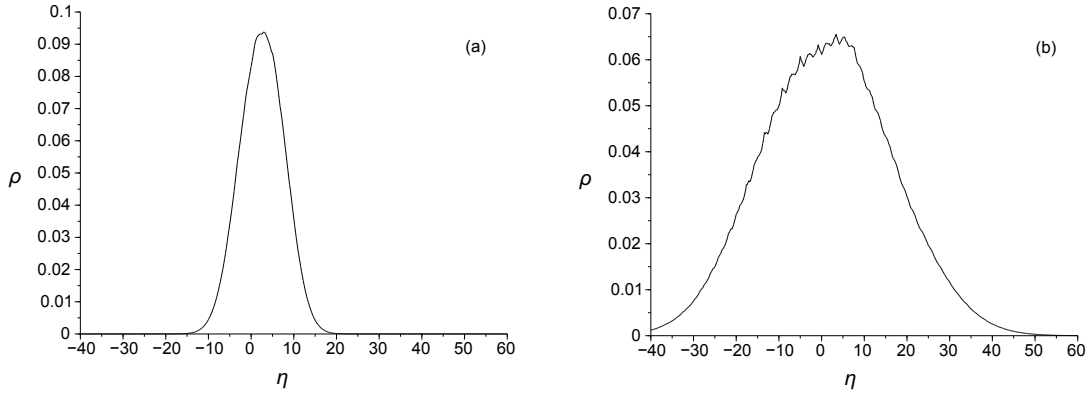


FIG. 9: Energy distribution at the end of the modulator for (a) $|a|^2 = 16$, (b) $|a|^2 = 289$.

III. FINAL COMMENTS

The results obtained so far confirm that the consequences of the heater interaction are more rich than usually believed [3, 7]. It seems indeed that the successive passage of the beam inside the Linac accelerating sections is such that it preserves some memory of the effects by the FEL dynamics inside the first undulator. The heater does not simply induces a Gaussian noise, but has non-trivial effects which mark the successive emission inside the modulator in a way reminiscent of the echo mechanism [11].

The Colson dimensionless amplitude $|a|$ is associated with the laser intensity I according to the identity [8, 12]¹

$$|a|^2 = 0.8\pi^4 X \quad (3.1)$$

$$X = \frac{I}{I_s}$$

where I_s is the FEL saturation intensity, which is in turn linked to the beam and undulator parameters by

$$I_s \left[\frac{MW}{cm^2} \right] \cong 6.9 \times 10^2 \left(\frac{\gamma}{N} \right)^4 \frac{1}{[\lambda_u [cm] K f_b(\xi)]^2}, \quad (3.2)$$

$$f_b(\xi) = J_0(\xi) - J_1(\xi), \quad \xi = \frac{1}{4} \frac{K^2}{1 + \frac{K^2}{2}}$$

¹ Even though the laser used in the heater is an external laser and not a FEL, we use the same formalism of self-induced heating because the effects are the same.

Using the parameters reported in ref. [7] for the heater section ($\gamma \cong 200$, $\lambda_u = 4\text{cm}$, $K = 1.17$, $N = 12$) we obtain for the saturation intensity of the heater section $I_s \cong 3 \times 10^6 \frac{\text{MW}}{\text{cm}^2}$. Using such a value as reference number we obtain that in correspondence of the first maximum of the third harmonic bunching coefficient, the corresponding laser intensity is $I \cong \frac{|a|^2}{0.8\pi^4} I_s = 0.6 \times 10^6 \frac{\text{MW}}{\text{cm}^2}$.

A comparison between the results presented in Figs. 5 and those reported in ref. [7] in terms of absolute energy values is made difficult, since our treatment does not include 3-D effects and we cannot determine the effective overlapping between electron and photon beams. A comparison is however possible if we adopt a different strategy. We “calibrate” the horizontal axis in Fig. 5 in such a way that the first maximum coincides with $1\mu\text{J}$. By overlapping the plot in Fig. 5a, with the experimental results concerning the FEL intensity at 32 nm in the radiator for the case of FERMI experiment, we obtain what has been reported in Fig. 10, the comparison is satisfactory, even though our calculation refers to the square modulus of the bunching coefficient at the end of the modulator and the experimental results to the FEL intensity at the end of three undulator sections in the radiator. In these conditions, being eliminated the gain effects, the output pulse intensity is directly proportional to the square modulus of the bunching coefficient itself. Therefore we normalize the peak bunching with the peak energy reported in ref. [7]. An important remark is that the analysis developed in this paper correctly predicts the low LH intensity behaviour and not only that at larger energy. To make the comparison more substantive we have reported in Fig. 11 the slice induced energy spread, in the heater section: we have interpolated our numerical results with the analytical formula [14]

$$\sigma(X) = \frac{0.433}{N} e^{-0.25\beta X + 0.01\beta^2 X^2} \sqrt{\frac{\beta X}{1 - e^{-\beta X}} - 1} \quad (3.3)$$

The comparison with the experimental results quoted in [13] provides quite a good agreement, which has been further checked using the numerical procedure based on the FPE equation.

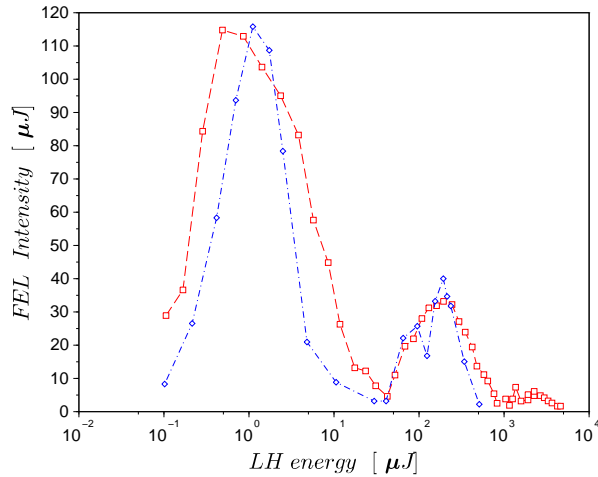


FIG. 10: Comparison between the results presented in Fig. 5a (blue diamond dashed-dot) and those reported in ref. [7] (red box dashed).

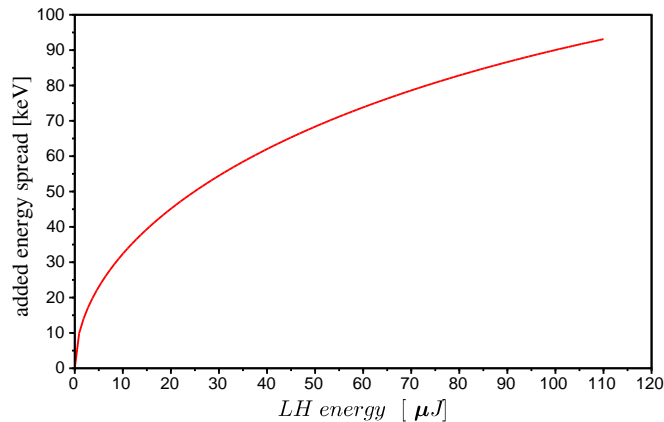


FIG. 11: The slice induced energy spread, in the heater section vs. LH energy

Since the amount of laser energy quoted in the experiment for the first peak is around $E_L \cong 1\mu J$, according to the characteristic of the laser for the FERMI heater reported in [7] (namely laser pulse duration $\tau_L \cong 10ps$, transverse section $\sigma_L \cong 0.2mm$) we can evaluate the laser pulse intensity corresponding to $I_L = \frac{E_L}{2\pi\sigma_L^2\tau} \cong 0.6\frac{MW}{cm^2}$. The second peak is predicted by our model to be determined by a laser energy larger by a factor 20 than that corresponding to the first.

The agreement between theory and experiment can be considered satisfactory.

We must underline that our treatment holds for large laser size compared to the e-beam, namely for $\sum_L \gg \sum_E$, when such a condition does not occur the energy distribution after the heater is more similar to a Gaussian. This aspect of the problem has however been thoroughly discussed in ref. [3] and will not be reconsidered here.

The analysis we have developed in the paper is straightforward from the conceptual point of view but rather heavy in terms of computer time.

To reduce the number of calculations we have simplified the part concerning the effect of the Landau Damping inside the Linac. We have assumed indeed a heuristic model implying that the heater energy induced distribution combines with that due to the wake field inside the Linac structures, becoming less efficient in providing additional spread with increasing heating noise. The model is essential that proposed in ref. [2].

It has been stressed that the occurrence of new maxima emerging in the bunching coefficients is associated with the fact that the energy distribution deviates from a Gaussian after the heater. We have considered the dependence on the heater energy of the average energy value, rms and of the Fisher index [15] defined as $\delta = \frac{m_4 - 3\sigma^4}{\sigma^4}$ (see Fig. 12). This last quantity measures the relevance of the dissymmetry and indeed it becomes more negative with increasing heater energy, as also evident by comparison with Fig. 9.

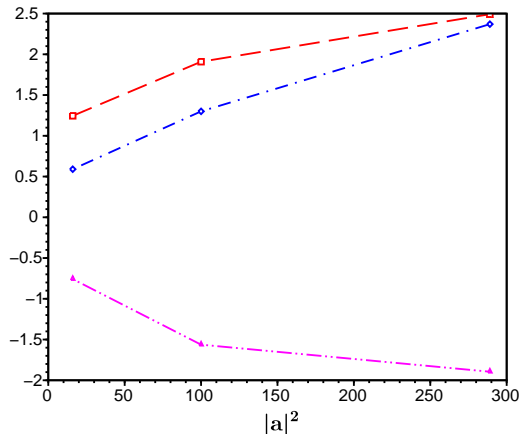


FIG. 12: First moment of the energy distribution (red square mark), second moment (blue diamond mark), Fisher parameter (magenta triangle mark). The second moment (namely the induced energy spread) has been divided by 10.

The analysis we have developed agrees fairly well with the experimental results even

though the modelling of the heater is rather simplified. We have used fairly general method which predicts that the effect of the recurrence of maxima is present also for higher order bunching coefficients, even though the peaks are significantly narrower. We also underline that the present analysis satisfactorily reproduces the whole trend of the curves from low to high heater energy. It is also worth stressing that the position of the peaks does not change dramatically with the heater energy (at least for odd harmonics). However, regarding the case of even order bunching coefficients, it seems that the structure of the peaks is different from that of the odd cases with the secondary maxima more pronounced and shifted towards higher energy values. At the moment we have no convincing explanation for such a behavior, which, if confirmed by the experiment, is still an open question.

Acknowledgements

The Authors express their sincere appreciation to L. Giannessi for a clarifying discussion on the results of ref. [7] and to T. Dubuc for the analysis of the experimental data.

-
- [1] Z. Huang et al., *Phys. Rev. ST Accel. Beams*, 13, 020703 (2010).
 - [2] E.L. Saldin, E.A. Schneidmiller, and M.V. Yurkov, *NIM A* 490, 1 (2002).
 - [3] Z. Huang et al. *Phys. Rev. ST Accel. Beams*,7, 074401 (2004).
 - [4] S. Heifets, S. Krinsky, G. Stupakov, “Coherent synchrotron radiation instability in a bunch compressor”, *Phys. Rev. ST Accel. Beams* 5, 064401 (2002).
 - [5] R. Bartolini, G. Dattoli, L. Mezi, A. Renieri, M. Migliorati, M. E. Couprie, G. De Ninno, and R. Roux, “Suppression of the Sawtooth Instability in a Storage Ring by Free-Electron Laser: An Example of Nonlinear Stabilization by Noise”, *Phys. Rev. Lett.* 87, 134801 (2001).
 - [6] G. Dattoli, M. Labat, M. Migliorati, P.L. Ottaviani, S. Pagnutti, E. Sabia, “The FEL SASE operation, bunch compression and the beam heater”, *Opt. Commun.* 284 (2011) p. 1945.
 - [7] E. Ferrari, E. Allaria, W. Fawley, L. Giannessi, Z. Huang, G. Penco, and S. Spampinati, “Impact of non-Gaussian electron energy heating upon the performance of a seeded free-electron laser”, accepted for publication 27 jan 2014.
 - [8] G. Dattoli, L. Giannessi, and A. Torre, “Unified view of free-electron laser dynamics and of higher-harmonics electron bunching”, *J. Opt. Soc. Am. B/Vol.* 10, No. 11 (1993).
 - [9] W B. Colson, in *Laser Handbook*, W B. Colson, C. Pellegrini, and A. Renieri eds. (North-

- Holland, Amsterdam, 1990), Vol. VI, p. 301.
- [10] G. Dattoli and E. Sabia, “Bunching coefficients in echo-enabled harmonic generation”, *Phys. Rev. ST Accel. Beams* 16, 070702 (2013).
 - [11] G. Stupakov, “Using the Beam-Echo Effect for Generation of Short-Wavelength Radiation”, *Phys. Rev. Lett.* 102, 074801 (2009).
 - [12] F. Ciocci, G. Dattoli, A. Torre, A. Renieri, “Insertion Devices for Synchrotron Radiation and Free Electron Laser”, World Scientific Publishing Co Pte Ltd, Singapore (2000).
 - [13] S. Spampinati et al., “Laser heater commissioning at an externally seeded free-electron laser”, *Phys. Rev. ST Accel. Beams* 17, 120705 (2014).
 - [14] G. Dattoli, P.L. Ottaviani, S. Pagnutti, “Booklet for FEL design: a collection of practical formulae”, ENEA Internal Report RT/2007/40/FIM (2007).
 - [15] R. A. Fisher, “Statistical methods for research workers” (14th ed.), Edinburgh, Scotland: Oliver & Boyd (1970).